Japanese Journal of Applied Physics **52** (2013) 07HE02 **REGULAR PAPER**
http://dx.doi.org/**10.7567/JJAP.52.07HE02**

Demonstration of Noncontact Ultrasonic Mixing of Droplets

Ryohei Nakamura, Yosuke Mizuno, and Kentaro Nakamura

Precision and Intelligence Laboratory, Tokyo Institute of Technology, Yokohama 226-8503, Japan

Received November 23, 2012; accepted January 29, 2013; published online June 20, 2013

The noncontact ultrasonic mixing of two droplets is demonstrated, for the first time, by controlling the acoustic field using the following two methods: (1) by changing the distance between the vibrator and the reflector and (2) by modulating the driving voltage amplitude applied to the vibrator. The operating principle is confirmed by measuring the acoustic pressure distribution and the temporal change in the acoustic pressure near the mixing position. We also show that the stable mixing of droplets with high repeatability is feasible by method (2), which does not involve the use of mechanically moving parts. © 2013 The Japan Society of Applied Physics

1. Introduction

In the biochemical, pharmaceutical, and new material industries, the noncontact transport of small components, powders, and liquids is highly demanded. Although a number of methods based on air pressure and electric/magnetic fields have been proposed, they suffer from noise, high cost, and applicability only to electric/magnetic objects.[1–11] To overcome these drawbacks, noncontact ultrasonic transport has been extensively studied so far, in which various ultrasonic technologies for manipulating small objects, particles, and cells in air[12–19] and in liquid are used.[20–22] We are currently aiming at implementing all of its procedures, i.e., injection, linear transport, direction switching, ejection, analysis, and dispensing, based on ultrasonics. When the materials to be transported are liquids (or droplets), mixing of multiple droplets is also essential. Up to now, linear transport,[23–25] direction switching,[26] and ejection[27] have been successfully demonstrated, but other procedures need to be developed to achieve our aim.

Here, we focus on the mixing of multiple droplets. Droplets trapped and levitated at some particular points can be mixed by controlling the acoustic field, as shown in Fig. 1, based on one of the following four methods: (1) by using traveling waves, (2) by switching the acoustic modes, (3) by changing the distance between the vibrator and the reflector, and (4) by modulating the driving voltage amplitude applied to the vibrator. In this study, we demonstrate the noncontact ultrasonic mixing of two droplets using methods (3) and (4). The operating principle is confirmed by measuring the acoustic pressure distribution and the temporal change in the acoustic pressure near the mixing position. Method (4), which does not involve the use of any mechanically moving parts, is shown to have a higher repeatability than method (3).

2. Experimental Procedure

Figure 2 shows the experimental setup, where a Langevin transducer with an exponential horn excited a breathing mode of an aluminum ring (vibrator) at 25.9 kHz, and an 85-mm-long acrylic cylinder (reflector) was fixed in the ring. The depth of the vibrator was 30 mm. As is shown in the next section, the acoustic field had one nodal circle and twelve radial nodal lines, as shown in Fig. 3. Here, we should note that the alignment of the nodal lines is not bilaterally symmetric due to the bolt cap shown in Fig. 2, and that objects are levitated at the position located along the

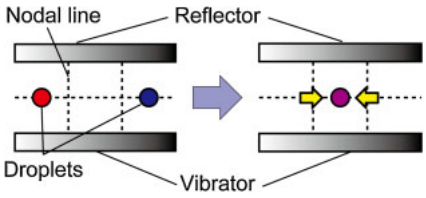

Fig. 1. (Color online) Concept of noncontact ultrasonic mixing of two droplets.

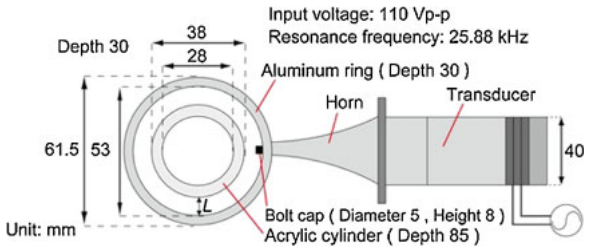

Fig. 2. (Color online) Experimental setup for droplet mixing.

nodal circle and at the midpoint of two neighboring nodal lines.[28] Water was converted into droplets, which were manually injected using a syringe into the acoustic field between the vibrator and the reflector, and levitated at two different points. The maximum volume of the droplet levitated with this setup was 19 µl.

2.1 Experiments (I): Change in vibrator/reflector distance

As the first trial, by shaking the vibrator in the vertical direction to change the distance between the vibrator and the reflector [which was initially set to 7 mm at an angular position of 90° (see Fig. 3)], we successfully demonstrated noncontact droplet mixing, as shown in Figs. 4(a)–4(d). The two droplets were (a) levitated at different points and (b) moved by changing the vibrator/reflector distance, until they (c) touched each other and (d) mixed using surface tension. In Fig. 4(a), the volume of the bottom droplet was 1.8 µl, and that of the other droplet was 0.4 µl. The mixed droplet was rotating, which apparently contributed to the stirring of its content.[29]

To confirm the operating principle of this method, the acoustic field distribution between the vibrator and the reflector was measured as the modulation in optical path

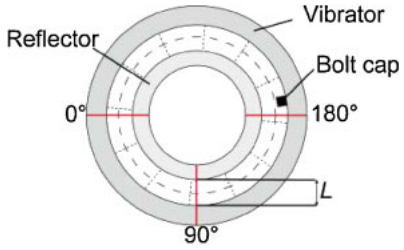

Fig. 3. (Color online) Schematic acoustic field. The dotted circle/lines indicate the nodal circle/lines.

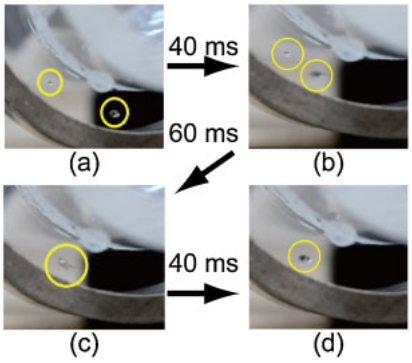

Fig. 4. (Color online) Photographs of droplet mixing by changing the vibrator/reflector distance: (a) two droplets levitated at different points, (b) two droplets approaching each other, (c) beginning of droplet mixing, and (d) mixed droplet.

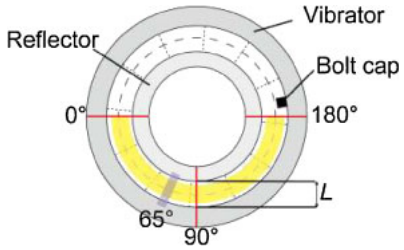

Fig. 5. (Color online) Two directions in which the acoustic field distribution and its dependence on the vibrator/reflector distance L were measured.

length using a laser Doppler vibrometer (LDV) with a wavelength of 633 nm. Considering the acoustooptic effect of air and the transformation of the path length modulation into the resultant LDV output, the acoustic pressure p is expressed as[30)]

$$p = \frac{n}{n-1}\frac{c^2\rho}{2\pi f l}v_{\mathrm{LDV}}, \quad (1)$$

where n is the refractive index of air (= 1.0002764), c the acoustic velocity (= 346.51 m/s at 25 °C), ρ the density of air (= 1.184 kg/m^3), f the frequency of the acoustic field, l the acoustic field length (= 30 mm), and v_{LDV} the velocity measured with the LDV. As shown in Fig. 5, the acoustic field distribution and its dependence on the vibrator/reflector distance L at 90° were measured in two directions: the circumferential direction from 0 to 180° and the radial

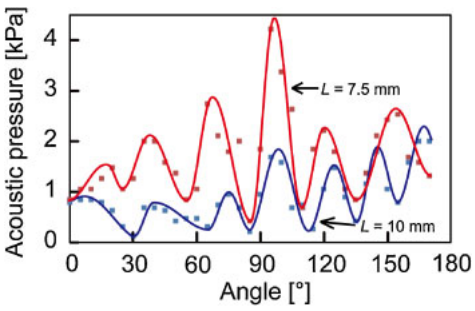

Fig. 6. (Color online) Measured circumferential acoustic pressure distribution when the L values were 7.5 and 10 mm.

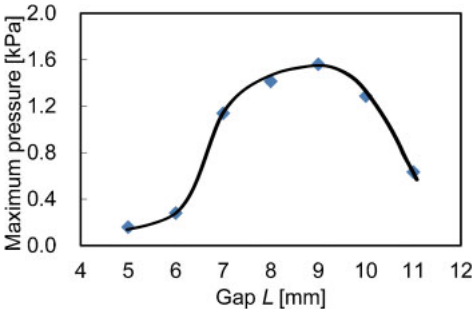

Fig. 7. (Color online) Measured maximum acoustic pressure in the radial direction at 65° vs L.

direction at 65° (where the droplets were mixed). In the circumferential direction, the acoustic pressure distribution was measured along the midline between the vibrator and the reflector; in the radial direction, first, the acoustic field distribution at 65° was measured, and then the maximum pressure was obtained at each L. Figure 6 shows the measured circumferential acoustic pressure distribution when the L values were 7.5 and 10 mm. As L was changed, the acoustic pressure also markedly changed, but the positions of the nodal points at approximately 90° only slightly changed. Figure 7 shows the measured maximum acoustic pressure in the radial direction at 65° as a function of L, which also indicated that the pressure was highly dependent on L. When L was approximately 9 mm, the maximum acoustic pressure was highest; when L was approximately 7 mm (experimentally employed), a marked change in the maximum pressure was observed. Thus, the operating principle of this method appears to be as follows: first, when the vibrating ring was shaken upward, L became shorter, and consequently the acoustic pressure applied to the droplets was temporarily reduced; then the droplets shifted in the circumferential direction with gravity and mixed with each other. When the vibrating ring returned to its initial position, the mixed droplet was also trapped at the initial position.

We also measured the vibration mode of the vibrator in the depth and circumferential directions with the LDV. The vibration velocity was almost uniform in the depth direction. The measured vibration velocity distribution in the circumferential direction is shown in Fig. 8, in which the number and positions of nodal points were inconsistent with those

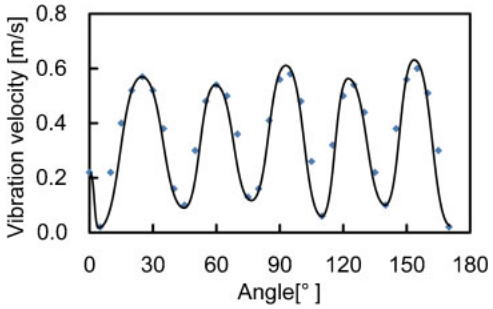

Fig. 8. (Color online) Measured vibration velocity distribution of vibrator in the circumferential direction.

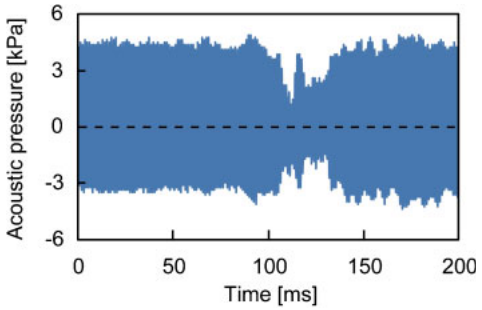

Fig. 9. (Color online) Measured temporal change in the acoustic pressure at the strongest antinode near the mixing position.

in Fig. 6. This indicates that the vibration modes of the vibrator and that of the air were different, resulting in the selective excitation of the vibration mode of the air, which is similar to that of the vibrator.

In addition, we measured the temporal change in the acoustic pressure at the strongest antinode near the position where the droplets were mixed, which is shown in Fig. 9. When the vibrating ring was shaken upward and L became shorter, the acoustic pressure was reduced; when the ring returned to its initial position, the pressure also returned to the initial value. The waveform was, however, distorted probably owing to the mechanical movement of the vibrator, resulting in poor repeatability. Other methods that involve no mechanical movement need to be developed to perform noncontact droplet mixing with higher stability.

2.2 Experiments (II): Amplitude modulation of driving voltage

Next, by periodically modulating the driving voltage amplitude applied to the vibrator (schematically shown in Fig. 10; modulation period: 50 ms), we demonstrated the noncontact mixing of two droplets, as shown in Figs. 11(a)–11(c). The two droplets were (a) levitated at different points, (b) moved by the amplitude modulation of the driving voltage, and finally (c) mixed. In Fig. 11(a), the volume of the bottom droplet was 1.5 µl and that of the other droplet was 0.4 µl. The mixed droplet kept on oscillating in the circumferential direction until the modulation was stopped.

The acoustic pressure distribution in the circumferential direction was the same as the curve when $L = 7.5$ mm in Fig. 6, because the distance between the vibrator and the

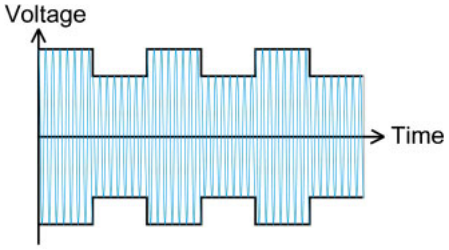

Fig. 10. (Color online) Schematic of periodical amplitude modulation applied to the driving voltage.

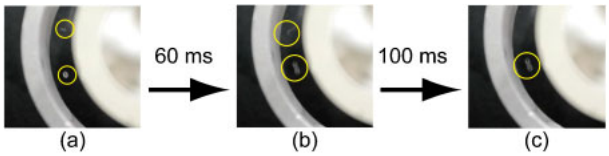

Fig. 11. (Color online) Photos of droplet mixing by amplitude modulation of the driving voltage: (a) two droplets levitated at the different points, (b) two droplets moving circumferentially, and (c) mixed droplet.

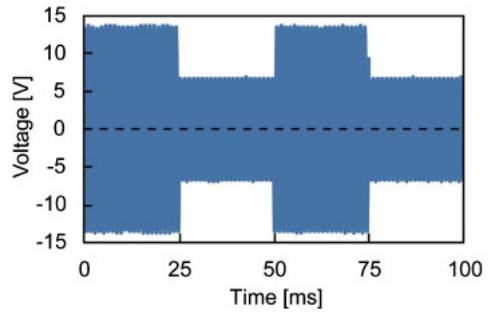

Fig. 12. (Color online) Measured temporal changes in (a) driving voltage applied to the vibrator and (b) acoustic pressure at the strongest antinode near the mixing position.

reflector was fixed at 7.5 mm in this experiment. The temporal change in the acoustic pressure at the strongest antinode near the mixing position was also measured. Figures 12(a) and 12(b) show the measured driving voltage applied to the vibrator and acoustic pressure as functions of time, respectively. Despite the abrupt change in the driving voltage amplitude, the corresponding change in the acoustic pressure was gradual with a time constant of ~10 ms, which might originate from the high quality factor of the vibration

system employed in the experiment. The quality factor was measured to be 925, corresponding to a time constant of 11.4 ms at 25.7 kHz, which is in good agreement with the results in Fig. 12(b).[31] Compared with the result described in the previous section (see Fig. 9), the waveform of the acoustic pressure was significantly improved with less distortion, which leads to a much higher repeatability. This is because the modulation-based method does not involve any mechanically moving parts.

3. Conclusions

We demonstrated the noncontact ultrasonic mixing of two droplets, for the first time, by controlling the acoustic field using two methods: by changing the distance between the vibrator and the reflector and by modulating the driving voltage amplitude applied to the vibrator. Then we confirmed their operating principle by measuring the acoustic pressure distribution and the temporal change in the acoustic pressure near the mixing position. We also showed that the stable mixing of droplets with a high repeatability can be performed by the modulation-based method, which does not involve the use of any mechanically moving parts. We think that our work is an important technological step toward the implementation of noncontact ultrasonic transport/analysis systems for droplets in the near future.

Acknowledgement

This work was partially supported by a Grant-in-Aid for Scientific Research (Challenging Exploratory Research, 23656163) from the Japan Society for the Promotion of Science (JSPS).

1) S. Konishi, M. Harada, Y. Ogami, Y. Daiho, Y. Mita, and H. Fujita: ETFA 6th Int. Conf., 1997, p. 232.
2) S. Mukhopadhyay, J. Donaldson, G. Sengupta, S. Yamada, C. Chakraborty, and D. Kacprzak: IEEE Trans. Magn. **39** (2003) 3220.
3) F. Hellman, E. M. Gyorgy, D. W. Johnson, H. M. O'Bryan, and R. C. Sherwood: J. Appl. Phys. **63** (1988) 447.
4) R. R. Whymark: Ultrasonics **13** (1975) 251.
5) E. G. Lierke: Acustica **82** (1996) 220.
6) H. Hatano, Y. Kanai, Y. Ikegami, T. Fujii, and K. Sato: Nihon Onkyo Gakkaishi **47** (1991) 40 [in Japanese].
7) E. Benes, M. Groschl, H. Nowotny, F. Trampler, T. K. Keijizer, H. Bohm, S. Radel, L. Gherardini, J. J. Hawkes, R. Konig, and C. Delouvroy: Proc. IEEE Ultrasonics Symp., 2001, p. 649.
8) Y. Hashimoto, Y. Koike, and S. Ueha: J. Acoust. Soc. Am. **103** (1998) 3230.
9) Y. Hashimoto, Y. Koike, and S. Ueha: J. Acoust. Soc. Am. **100** (1996) 2057.
10) R. Yano, M. Aoyagi, H. Tamura, and T. Takano: Jpn. J. Appl. Phys. **50** (2011) 07HE29.
11) Y. Yamayoshi and S. Hirose: Jpn. J. Appl. Phys. **50** (2011) 07HE28.
12) A. Haake and J. Dual: Ultrasonics **42** (2004) 75.
13) T. Kozuka, K. Yasui, T. Tuziuti, A. Towada, and Y. Iida: Jpn. J. Appl. Phys. **46** (2007) 4948.
14) T. Kozuka, K. Yasui, T. Tuziuti, A. Towada, and Y. Iida: Jpn. J. Appl. Phys. **47** (2008) 4336.
15) J. Hawkes, J. Cefai, D. Barrow, W. Coakley, and L. Briarty: J. Phys. D **31** (1998) 1673.
16) W. Coakley, J. Hawkes, M. Sobanski, C. Cousins, and J. Spengler: Ultrasonics **38** (2000) 638.
17) A. Haake and J. Dual: J. Acoust. Soc. Am. **117** (2005) 2752.
18) A. Osumi, K. Doi, and Y. Ito: Jpn. J. Appl. Phys. **50** (2011) 07HE30.
19) K. Matsumoto and H. Miura: Jpn. J. Appl. Phys. **51** (2012) 07GE05.
20) T. Kozuka, K. Yasui, S. Hatanaka, T. Tuziuti, K. Suzuki, and A. Towata: Jpn. J. Appl. Phys. **50** (2011) 07HE27.
21) K. Masuda, R. Nakamoto, N. Watarai, R. Koda, Y. Taguchi, T. Kozuka, Y. Miyamoto, T. Kakimoto, S. Enosawa, and T. Chiba: Jpn. J. Appl. Phys. **50** (2011) 07HF11.
22) M. Takeuchi and K. Yamanouchi: Jpn. J. Appl. Phys. **33** (1994) 3045.
23) D. Koyama and K. Nakamura: IEEE Trans. Ultrason. Ferroelectr. Freq. Control **57** (2010) 1152.
24) Y. Ito, D. Koyama, and K. Nakamura: Acoust. Sci. Technol. **31** (2010) 420.
25) M. Ding, D. Koyama, and K. Nakamura: Appl. Phys. Express **5** (2012) 097301.
26) D. Koyama and K. Nakamura: IEEE Trans. Ultrason. Ferroelectr. Freq. Control **57** (2010) 1434.
27) S. Murakami, D. Koyama, and K. Nakamura: AIP Conf. Proc. **1433** (2011) 783.
28) H. Miura: Nihon Onkyo Gakkaishi **47** (1991) 941 [in Japanese].
29) T. Otsuka and T. Nakane: Jpn. J. Appl. Phys. **41** (2002) 3259.
30) K. Nakamura, M. Hirayama, and S. Ueha: Proc. IEEE Ultrasonics Symp., 2002, p. 609.
31) M. Umeda, K. Nakamura, and S. Ueha: Jpn. J. Appl. Phys. **37** (1998) 5322.